

Scintillation properties of $\text{Lu}_3\text{Al}_{5-x}\text{Sc}_x\text{O}_{12}$ crystals

This article has been downloaded from IOPscience. Please scroll down to see the full text article.

1994 J. Phys.: Condens. Matter 6 10423

(<http://iopscience.iop.org/0953-8984/6/47/025>)

View [the table of contents for this issue](#), or go to the [journal homepage](#) for more

Download details:

IP Address: 171.66.16.179

The article was downloaded on 13/05/2010 at 11:24

Please note that [terms and conditions apply](#).

Scintillation properties of $\text{Lu}_3\text{Al}_{5-x}\text{Sc}_x\text{O}_{12}$ crystals

N N Ryskin†, P Dorenbos†, C W E van Eijk† and S Kh Batygov‡

† Delft University of Technology, Faculty of Applied Physics, c/o IRI, Mekelweg 15, 2629 JB Delft, The Netherlands

‡ General Physics Institute, 117313 Vavilov Street 38, Moscow, Russia

Received 16 August 1994

Abstract. The scintillation properties of $\text{Lu}_3\text{Al}_{5-x}\text{Sc}_x\text{O}_{12}$ single garnet crystals doped with different concentrations of Sc^{3+} were investigated. The best scintillation properties were obtained for the crystal with $x = 0.2$ in the melt. This crystal has a broad (FWHM ~ 1 eV) ultraviolet emission band with a maximum at 275 nm. An energy resolution of 7% is observed for the 662 keV photopeak. The main decay component of the scintillation pulse has an exponential decay time of about 600 ns and accounts for 90% of the total light yield. The total scintillation light yield was found to be about 22 500 photons/MeV. Within 10% a linear response was obtained in the energy interval from 8 keV to 1.3 MeV. The energy resolution was found to be approximately inversely proportional to the square root of the excitation energy.

1. Introduction

$\text{Lu}_3\text{Al}_5\text{O}_{12}$ garnet crystals (hereinafter referred to as LAG), due to their high density (6.67 g cm^{-3}) and other physical properties such as shock resistivity, non-hygroscopicity and chemical radiation stability, are known to be quite promising host crystals for scintillating materials. Earlier [1], scintillation properties of LAG crystals doped with Ce^{3+} ions were reported. Two emission bands with maxima at 300 nm caused by intrinsic luminescence of pure LAG and at 530 nm caused by luminescence of Ce^{3+} ions with a light yield of 3000 photons/MeV and 11 000 photons/MeV, respectively, were observed at room temperature under x-ray excitation. It was also shown [2] that substitution of Al^{3+} ions by Sc^{3+} ions in the LAG lattice gives rise to a broad (FWHM ~ 1 eV) ultraviolet (UV) band located near 280 nm at room temperature. Occurrence of new luminescence bands in the UV region when Sc^{3+} ions are introduced into yttrium–aluminium garnet (YAG) crystals has been observed in [3–5] and was assigned to the formation of effective luminescence centres by Sc^{3+} ions. Sc^{3+} ions in YAG or LAG) are isoelectronic impurities with a closed-shell configuration. They do not show radiative transitions, as do, for instance, Ce^{3+} and the other lanthanide ions (except for La^{3+} and Lu^{3+}). However they may form effective centres for radiative recombination of electrons and holes due to differences between ionic radii of Sc^{3+} ions and the substituted ions.

In the present paper, results of an investigation of the scintillation properties of LAG crystals doped with Sc^{3+} ions are presented.

2. Experimental procedure

The crystals investigated in this work were grown by the horizontally directed crystallization technique in Mo crucibles under vacuum. The Sc^{3+} concentration in the samples was

determined by means of electron probe microanalysis. The relationship between Sc^{3+} content in the melt and in the bulk crystal is presented in table 1. From this point on we shall use those values of the Sc^{3+} concentration presented in the first column of table 1. The samples were found to be colourless and of good quality. However at high Sc^{3+} concentration (more than $x = 0.5$ in the melt) one could observe heterogenous parts in the bulk, which probably may be connected with the presence of other crystallographic phases. The samples were cut and polished on both sides except for the sample with $x = 2.0$, which was polished only on one side. Samples with dimensions of 5×5 – 7×7 mm² and of 1.0 mm thickness were used for the experiments.

Table 1. The position of emission maxima, the FWHM of the emission band and the light yield of $\text{Lu}_3\text{Al}_{5-x}\text{Sc}_x\text{O}_{12}$ garnet crystals as a function of the Sc concentration x under x-ray excitation, 35 kV, 25 mA, Cu anode, $T = 300$ K.

x in the melt	x in the crystals	λ_{max} (nm)	FWHM (eV)	Light yield (ph MeV ⁻¹)
0.001	0.006	293	1.43	14 400
0.04	0.04	273	1.10	18 500
0.2	0.16	275	1.01	22 400
0.5	0.42	282	1.09	23 800
2.0	1.3	340	1.03	17 600

To obtain x-ray excited luminescence spectra, the crystals were irradiated through a Be window with x-rays from an x-ray tube with a Cu anode operated at 35 kV and at 25 mA. Light from the samples was monitored within the range from 120 nm to 540 nm by means of a scanning monochromator (Acton Research Corporation ARC model VM-502) and a Thorn EMI (type 9426B) photomultiplier tube (PMT). The emission spectra were corrected for the recording system response. The emission intensity was compared with the intensity from a pure BaF_2 crystal of about the same dimensions and also with both faces polished. This crystal has a well determined light yield of about 11 000 photons/MeV of absorbed x-ray energy, which provides a calibration of the emission spectra in units of photons/MeV nm⁻¹.

Optical transmission spectra in the interval from 190 nm to 820 nm were recorded by means of a Hewlett Packard type HP 8452A diode array spectrophotometer with a wavelength resolution of 2 nm.

For determining the absolute and relative light yield, a crystal is mounted with an optical coupling compound (Viscasil 60 000 cSt from General Electric) to the window of a Philips XP2020Q photomultiplier tube with a CERN type 4238 voltage divider. To optimize the light collection the crystal was covered with several layers of 0.1 mm thick UV reflecting Teflon tape. The absolute photoelectron yield was obtained by comparing the location of the 662 keV photopeak in the pulse height spectrum of a ¹³⁷Cs source with the location of the maximum in the pulse height spectrum of single photoelectrons from the photocathode.

We used ²⁴¹Am, ¹⁰⁹Cd, ⁵⁷Co, ¹³³Ba, ¹³⁷Cs, ²²Na and ⁶⁰Co γ -ray sources to excite the crystals at energies between 59 keV and 1.332 keV. An Amersham (code AMC.2084) variable x-ray source was employed to excite the samples at energies between 8 keV and 44.5 keV. In this source, ²⁴¹Am produces characteristic $K\alpha$ and $K\beta$ x-rays from Cu, Rb, Mo, Ag, Ba and Tb targets.

Pulse height spectra of the above excitation sources were recorded using an EG&G Ortec (model 672) spectroscopy amplifier. The relative light yield was then obtained

by comparing the position of the photopeak at a certain energy with the position of the photopeak at energy 662 keV in the pulse height spectrum of a ^{137}Cs source. Since the gain of the PMT appears to depend slightly on the anode current, which in turn is determined by the intensity and the efficiency of the scintillator, it was sometimes necessary to correct for such gain differences. The relative gain was determined from pulse height spectra of single electrons from the photocathode.

Decay time measurements were carried out with a LeCroy LS140 oscilloscope station. A scintillation pulse from a crystal mounted on an XP2020Q PMT was immediately fed to a 50 Ω loaded input of the oscilloscope station. In the case of the LAG-Sc ($x = 0.2$) crystal, the decay time spectrum was measured by means of the single-photon counting technique also. The scintillation pulse from the crystal mounted on the so-called start PMT (XP2020Q) provides a start pulse for a LeCroy 4208 time digital converter (TDC). A second PMT (which is also an XP2020Q) observes the same scintillation pulse via some adjustable slit. Only a few single photons from the scintillation event are observed by this so-called stop PMT, which provides the multiple stops for the TDC.

A vacuum ultraviolet (VUV) excitation set-up was used to measure excitation and emission spectra of the LAG-Sc ($x = 0.2$) sample. In this set-up the light of an ARC DS-775 deuterium lamp is passed through an ARC VM-502 vacuum monochromator and focused on the sample using an MgF_2 lens. The light emitted by the sample is collected by a quartz lens and monitored using a Jobin-Yvon H10 UV monochromator and a PMT (Philips XP2020Q). The spectra were corrected for the spectrum of the light source and transmission of the system using sodium salicylate as a reference. In this way excitation and emission measurements can be varied from 130 nm to 370 nm, and from 180 nm to 600 nm, respectively. More details on the experiments described above can be found in [6-8].

3. Results and discussion

X-ray excited luminescence spectra of LAG-Sc crystals with different Sc^{3+} concentrations are shown in figure 1. Each spectrum exhibits a broad UV emission band. The position of maximal emission, the FWHM of the band, and the integral light yield are listed in table 1. Besides these broad bands one observes (especially at low Sc^{3+} concentration) narrow peaks connected with uncontrolled impurities of rare earth elements, such as Gd^{3+} emission in the vicinity of 314 nm ($^6\text{P}_{7/2} \rightarrow ^8\text{S}_{7/2}$), Tb^{3+} emission lines at 384, 418 and 437 nm ($^5\text{D}_3 \rightarrow ^7\text{F}_6$, $^7\text{F}_5$ and $^7\text{F}_4$, respectively), as well as two small peaks of Nd^{3+} emission at approximately 400 nm. The latter is due to the transitions from the $^2\text{F}_{25/2}$ level to the $^4\text{F}_{9/2}$ and $^2\text{H}_{29/2}$ levels of Nd^{3+} . The slight increase of intensity in the spectra occurring at wavelengths longer than 500 nm is caused by the second-order reflection of the grating in the monochromator. As can be seen in figure 1 as well as in table 1, the position of the maxima of the spectra shifts with Sc^{3+} concentration. The position at first shifts to shorter wavelengths with a simultaneous decrease of the FWHM, and then (at a concentration higher than $x = 0.2$) to longer wavelengths with a simultaneous increase of the FWHM. The light yield was found to be highest and almost the same (taking into account the 10% error) for LAG-Sc samples with Sc^{3+} concentrations of $x = 0.2$ and $x = 0.5$.

The temperature dependence of the intensity of the UV emission of LAG-Sc ($x = 0.5$) at two different wavelengths (250 nm and 330 nm) is shown in figure 2. For a better understanding of these temperature dependences, it is necessary to discuss experimental data and considerations given in [2] and [9]. As was shown in [2] x-ray excited luminescence

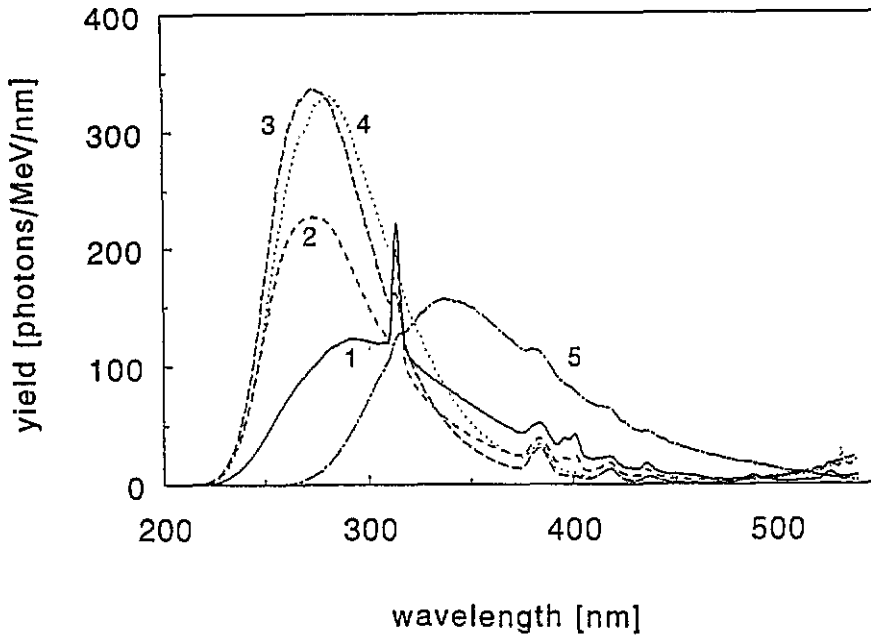


Figure 1. X-ray excited luminescence spectra of $\text{Lu}_3\text{Al}_{5-x}\text{Sc}_x\text{O}_{12}$ at room temperature: (1) $x = 0.001$, (2) $x = 0.04$, (3) $x = 0.2$, (4) $x = 0.5$, (5) $x = 2.0$.

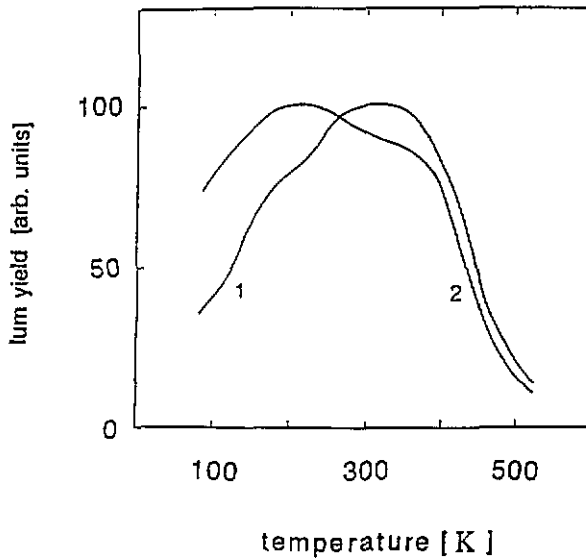


Figure 2. Temperature dependences of the UV emission of LAG-Sc ($x = 0.5$) at different wavelengths: (1) 250 nm, (2) 330 nm, normalized to 100 at the maxima of the curves.

spectra of undoped LAG consist of at least two main UV bands (FWHM ~ 0.8 eV): (i) a short-wavelength (SW) band with a maximum in the vicinity of 260–270 nm and (ii) a

long-wavelength (LW) band with a maximum at approximately 295–300 nm. It should be noted that these properties of undoped LAG are almost the same as those of undoped YAG (see for instance [10], [11]). Therefore there could be at least three UV bands in the x-ray excited luminescence spectra of LAG–Sc crystals at Sc^{3+} concentration lower than $x = 0.5$: two UV bands related to undoped LAG, and one UV band related to the Sc^{3+} ions (hereinafter named the Sc^{3+} band) with an intermediate position of the maximum ($\lambda_m \approx 275$ nm) in the spectra. The relative intensities of the three bands determine the FWHM and position of the resulting broad emission band.

Table 2. Time characteristics of the scintillation decay curves and the relative initial intensity I_0 (%) of $\text{Lu}_3\text{Al}_5-x\text{Sc}_x\text{O}_{12}$ garnet crystals measured with an oscilloscope station (LeCroy LS140) at room temperature.

x	Fast component		Slow component	
	τ (ns)	I_0 (%)	τ (ns)	I_0 (%)
0.001	1000	70	4500	30
0.04	750	85	5000	15
0.2 ^a	610	97.7	3300	2.3
0.5	760	92	5000	8
2.0	850	90	7500	10

^a Obtained with the single-photon counting technique.

The experimental data on decay time measurements with the LAG–Sc crystals are listed in table 2. The scintillation decay curves show at least two components, called the fast and the slow ones. In some cases a very slow component could be found in the decay curves. The decay time of both the fast and the slow components of LAG–Sc is the smallest for $x = 0.2$. The very slow component is quite insignificant for $x = 0.2$. The decay curve could be fitted quite well with a sum of two exponential components: $\tau_1 \approx 610$ ns and $\tau_2 \approx 3300$ ns. The relationship (as a percentage) between the initial intensities (at time $t = 0$) of the fast and slow components is also given in table 2. As can be seen from table 2 the highest percentage of the fast component (97.7% of the total initial intensity I_0 at $t = 0$) was observed in LAG–Sc at $x = 0.2$. The corresponding relationship between the integral intensities of the fast and the slow component is 89/11.

The experimental data, and the considerations mentioned above, show that the scintillation properties of LAG–Sc ($x = 0.2$) are the most promising from the standpoint of research of new scintillator materials. We therefore concentrated our efforts to obtain information about this sample.

The excitation, emission and absorption spectra of LAG–Sc ($x = 0.2$) are shown in figure 3. The absorption spectrum (figure 3, curve 3) indicates two absorption bands at approximately 220 nm and 270 nm. Excitation in the 220 nm band gives rise to a weak broad emission band at about 400 nm, while the excitation in the 270 nm band does not yield an emission band. Probably these two absorption bands are connected with uncontrolled impurities of transition metal ions (e.g. Fe or Mn), or, as suggested in [12] for YAG crystals, with F-like colour centres. The absorption rises strongly at wavelengths shorter than 200 nm. By analogy with YAG, a band gap of about 8.0 eV can be assumed for LAG. As can be seen from figure 3 (curve 1) and figure 1, the 275 nm emission band under UV excitation looks the same as that under x-ray excitation. Moreover this band is excited at energies above the absorption edge (figure 3, curve 2), and is therefore considered to be intrinsic to the host crystal. The excitation spectrum of LAG–Sc ($x = 0.2$) depicts within the range from

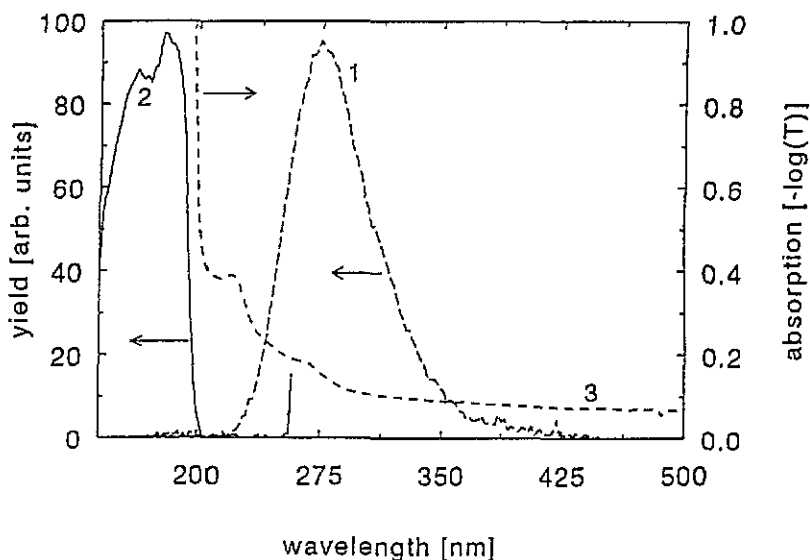


Figure 3. The emission (1), excitation (2) and absorption (3) spectra recorded for the LAG-Sc ($x = 0.2$) crystal at 300 K. (1) $\lambda_{ex} = 180$ nm, $\lambda_{em} = 200$ –450 nm. (2) $\lambda_{ex} = 140$ –250 nm, $\lambda_{em} = 275$ nm.

140 nm to 250 nm two relatively broad bands with maxima at about 160 and 180 nm. This excitation spectrum is closely similar to those obtained both with pure YAG crystals [13] for the SW emission band with a maximum at about 255 nm at 80 K (note that this band was assigned in that paper to self-trapped exciton emission) and with YAG-Sc crystals under synchrotron irradiation at room temperature [14]. These facts also indicate an exciton-like nature of the 275 nm emission band in LAG-Sc ($x = 0.2$).

A decay curve observed with the LAG-Sc ($x = 0.2$) crystal by means of the single-photon counting method is presented in figure 4. The properties of the decay curve have already been described. Whether the two decay components with $\tau_{fast} \approx 610$ ns and $\tau_{slow} \approx 3300$ ns are a feature of only a single luminescence band or are the characteristics of different luminescence centres is not clear yet. Moreover the slow component may be caused by a recombination process involving releasing of charge carriers from traps. Occurrence of a slow component in the decay curve of Ce^{3+} emission due to such release was observed in YAG-Ce [15]. To clarify this, further experiments should be carried out.

A pulse height spectrum of a ^{137}Cs γ -ray source obtained with the LAG-Sc ($x = 0.2$) crystal is shown in figure 5. From the photopeak at 662 keV, an energy resolution of 7% with a yield of 3490 photoelectrons/MeV (phe/MeV) was obtained. The absolute light yield Y in photons per megaelectronvolt (photon/MeV) can be obtained from the photoelectron yield by taking into account the quantum efficiency of the PMT, which is about 20% near 300 nm, and light collection losses of 5–10% [6]. It is necessary to point out that the average value of the photoelectron yield obtained with four independent measurements (3350, 3450, 3490 and 3550 phe/MeV) was found to be about 3460 phe/MeV. The spectrum was fitted within the region from 530 to 750 keV with two Gaussian peaks and a background. Together with the photopeak at 662 keV, the characteristic x-ray escape peak of Lu (the main x-ray emission of Lu lies at 54.07 keV) at an energy of 608 keV can be seen. It should be noted that the FWHM of the characteristic x-ray escape peak of Lu is slightly greater than that of the

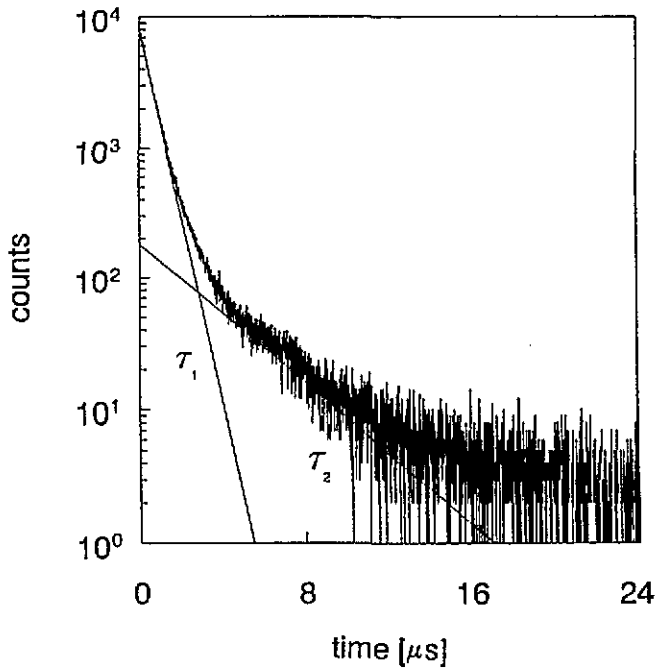


Figure 4. The 662 keV gamma ray excited decay curve of LAG-Sc ($x = 0.2$) obtained with the single-photon counting technique at 300 K. The straight lines represent exponentially decaying functions with decay times $\tau_1 = 610$ ns and $\tau_2 = 3300$ ns.

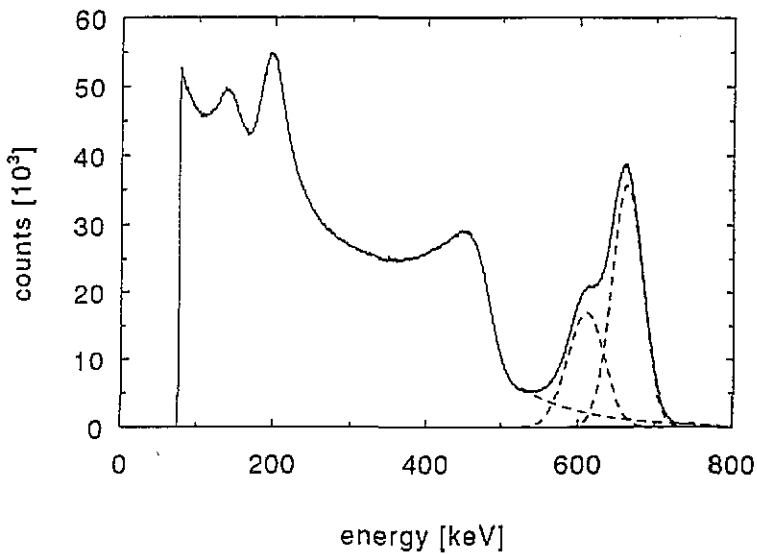


Figure 5. Pulse height spectrum of ^{137}Cs ($E_\gamma = 662$ keV) measured with the $1.0 \times 10 \times 15$ mm 2 LAG-Sc ($x = 0.2$) crystal at room temperature using a shaping time of 2 μs .

photopeak. This can be explained partly by the fact that besides the main characteristic $K\alpha_1$ x-ray emission of Lu at 54.07 keV there is the $K\alpha_2$ x-ray emission of Lu at 52.97 keV with 57% relative intensity. Figure 5 shows also two peaks within the interval from 100 keV to 250 keV. One of them, at an energy of about 195 keV, is identified as the Compton backscatter peak. The second peak, at about 136 keV, is the Lu x-ray escape peak related to the 195 keV backscatter peak.

Table 3. The photoelectron yield and the energy resolution at 662 keV versus the Sc^{3+} concentration x and the shaping time obtained from the pulse height spectra of a ^{137}Cs source at room temperature recorded with an XP2020Q photomultiplier tube.

x	Photoelectron yield (phe/MeV $^{-1}$)		Energy resolution with 662 keV excitation (%)	
	2 μs	10 μs	2 μs	10 μs
0.001	1200	1950	22.7	20.3
0.04	1750	2450	20	16.6
0.2	3450	4150	7	7.7
0.5	3350	3900	16.4	15.6
2.0	650	1000	24	25.4

The photoelectron yield and energy resolution obtained with a 2 μs and a 10 μs shaping time versus Sc^{3+} concentration under 662 keV excitation are presented in table 3. The best energy resolution and the highest yield were found for LAG-Sc ($x = 0.2$). It should be pointed out that in table 3 the average values are compiled. The best energy resolution obtained in our experiment with the LAG-Sc ($x = 0.2$) crystal under 662 keV excitation was found to be equal to 6.3%. This value is about the same as reported for the 'best' scintillator NaI-Tl. This is quite unexpected taking into account the fact that the light yield of NaI-Tl is almost twice as high as that of LAG-Sc ($x = 0.2$). It is probably related to the fact that the light yield as a function of the incident energy has a better linearity for LAG-Sc ($x = 0.2$) than for NaI-Tl.

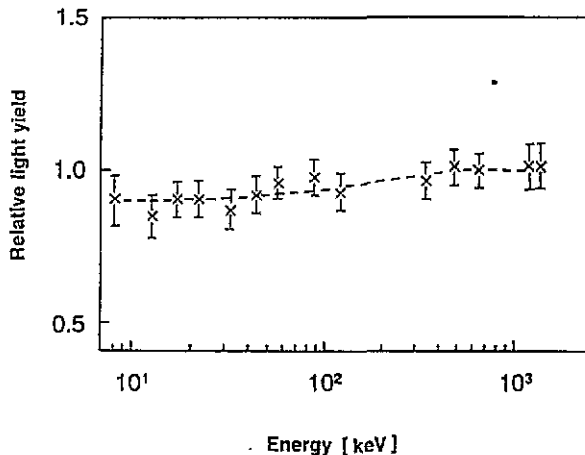


Figure 6. Light yield of LAG-Sc ($x = 0.2$) at room temperature versus excitation energy relative to the light yield at 662 keV.

The light yield (recorded with a 2 μs shaping time) of LAG-Sc ($x = 0.2$) relative to the light yield observed at 662 keV is plotted as a function of excitation energy in figure 6. Within the energy interval from 8 keV to 1.3 MeV one can see a value within 10% constant, i.e. a linear response within 10%. This linearity is considerably better than those observed for CsI-Tl, NaI-Tl, $\text{Lu}_2\text{SiO}_5\text{-Ce}$ (LSO-Ce), and $\text{Gd}_2\text{SiO}_5\text{-Ce}$ (GSO-Ce) [16, 17].

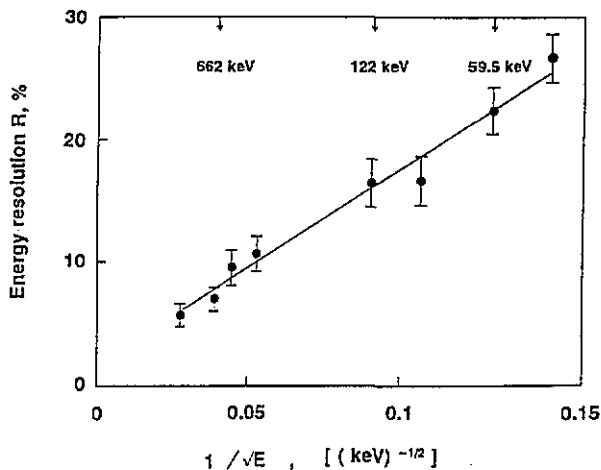


Figure 7. The energy resolution R (FWHM) obtained with LAG-Sc ($x = 0.2$) as a function of the inverse square root of the excitation energy.

Figure 7 shows the experimental energy resolution R (defined as the FWHM of a photopeak divided by the average pulse height H_0) obtained with the LAG-Sc ($x = 0.2$) crystal as a function of the excitation energy. If the scintillation process follows Poisson statistics then [16]

$$R = 2.35/\sqrt{N} = 1.26/\sqrt{E} \quad (1)$$

where N is the average number of photoelectrons generated per scintillation pulse, which for the crystal with $x = 0.2$ is equal to $3.46 \times E$ (keV). The fact that the solid line in figure 7 has a slope of 1.7 instead of 1.26 indicates a deviation from Poisson statistics. As pointed out [17], a contribution to R related to non-linearities in the scintillation response may play a significant role in the energy resolution of a scintillator. For example, the best energy resolution observed so far for LSO-Ce crystals amounts to about 9% at 662 keV excitation despite the fact that the total light yield is higher than that of LAG-Sc ($x = 0.2$). The same situation is observed with NaI-Tl, which shows a total light yield output twice as high as that of LAG-Sc. However the energy resolution at 662 keV of NaI-Tl and LAG-Sc ($x = 0.2$) is practically the same. This means that the non-statistical contribution to the energy resolution of LAG-Sc ($x = 0.2$) is the least compared with those of the crystals mentioned above. In its turn this fact is probably connected with the good linearity of LAG-Sc ($x = 0.2$).

As for the nature of the luminescent centres determining the UV emission of LAG-Sc ($x = 0.2$) it is reasonable to assume that this emission is due to luminescent centres formed by Sc^{3+} ions that substitute Al^{3+} ions in octahedral sites of the garnet structure. The suggestion that Sc^{3+} ions at low Sc content in LAG-Sc (up to about $x = 0.5$) enter the

octahedral sites of the lattice can be confirmed with the following considerations. Amongst the three cation sites (dodecahedral, octahedral and tetrahedral) of the garnet structure the latter sites are too small for Sc^{3+} . The ionic radii of Lu^{3+} in dodecahedral sites and Sc^{3+} and Al^{3+} ions in octahedral sites are 0.97 Å, 0.75 Å and 0.53 Å, respectively (i.e. the absolute differences between the ionic radii of Lu^{3+} and Sc^{3+} ions on the one hand and of Al^{3+} and Sc^{3+} ions on the other hand are the same). Consequently, Sc^{3+} ions may enter both the octahedral sites and dodecahedral ones. However a small number (up to about $x = 0.2$) of stoichiometric defects such as Y ions or Lu ions in octahedral sites have been proved [18] to be present in the garnet crystals grown by high-temperature methods. Therefore one may conclude that at low Sc concentrations the octahedral sites are the most preferable for Sc^{3+} ions. Certainly more convincing evidence may be obtained with measurements of the lattice constant of the LAG–Sc crystals. According to the considerations given above, at low concentration an increase of the lattice constant with increasing Sc concentration is to be expected, due to substitution of Al^{3+} by the larger Sc^{3+} . At high Sc concentration (more than about $x = 0.5$) when Sc^{3+} starts to substitute Lu^{3+} ions in dodecahedral sites one may expect a decrease of the lattice constant. Perhaps the luminescence band observed for LAG–Sc with $x = 2.0$ (see figure 1) with a maximum at 330 nm is due to luminescent centres formed by Sc^{3+} ions in dodecahedral sites of the LAG lattice. Moreover it was suggested [4] that at a high Sc concentration in YAG–Sc, emission due to donor–acceptor pairs is possible. In this case neighbouring Sc^{3+} ions in octahedral and dodecahedral sites are considered to trap a hole and an electron, respectively. It should be noted that the emission of such isoelectronic impurity centres has already been observed in semiconductors [19] and alkaline halide crystals [20]. According to the model suggested in [21] this luminescence is due to radiative relaxation of excitons bound near an isoelectronic impurity centre. At first one carrier is captured by an isoelectronic impurity centre due to a short-range potential and then an opposite-sign carrier is captured by the Coulomb potential (formed by the first carrier). An excited excitonic state is created, which leads to the emission of a photon. However a well developed theory describing such phenomena has not been reported yet.

The simplest model of excitation and relaxation processes occurring in LAG–Sc ($x = 0.2$) under ionizing radiation can be assumed as follows. Excitation by ionizing radiation or excitation with VUV light in the excitonic range leads eventually to formation of free excitons (or/and electron–hole pairs). Then an exciton (or/and an electron–hole pair) localize near an Sc^{3+} isoelectronic centre via the localization of the hole component. The radiative annihilation of such bound excitons gives rise to the 275 nm emission. It is necessary to point out that further investigations, both experimental and theoretical, should be carried out to obtain clearer insight into the processes connected with the luminescent properties of the isoelectronic impurities.

4. Conclusion

The scintillation properties of LAG–Sc crystals with the general formula $\text{Lu}_3\text{Al}_{5-x}\text{Sc}_x\text{O}_{12}$ with Sc concentrations from $x = 0.001$ to $x = 2.0$ (in the melt) have been investigated at room temperature for the first time.

On the basis of these investigations the following conclusions can be made.

(i) The best scintillation properties were found for an LAG–Sc crystal with an Sc concentration of $x = 0.2$.

(ii) Under x-ray excitation (35 kV, 25 mA, Cu anode) a wide (FWHM ~ 1 eV) UV luminescence band located at 275 nm is observed with LAG–Sc ($x = 0.2$), showing a total light yield of about 22 500 photons/MeV.

(iii) The UV band is excited at energies above the absorption edge, which is located at wavelengths shorter than 200 nm.

(iv) According to previous investigations this band starts to quench thermally at about 350 K.

(v) The decay curve of LAG-Sc ($x = 0.2$) can be fitted quite well with a sum of two exponential components: a fast one with a decay time $\tau_{\text{fast}} \approx 610$ ns (89% of the total integral intensity) and a slow one with a decay time $\tau_{\text{slow}} \approx 3300$ ns (11% of the total integral intensity).

(vi) From the pulse height spectra recorded with a ^{137}Cs source, total photoelectron yields of 3500 phe/MeV and 4150 phe/MeV with a corresponding energy resolution of about 7% and 7.7% were obtained using a 2 μs and 10 μs shaping time, respectively.

(vii) Within 10%, linearity was observed in the energy interval from 8 keV to 1.3 MeV.

(viii) The energy resolution of LAG-Sc ($x = 0.2$) was shown to be approximately inversely proportional to the square root of the excitation energy.

(ix) We propose that the UV luminescent band of LAG-Sc ($x = 0.2$) is of exciton-like nature and is caused by radiative recombination of an electron with a hole localized near a hole centre Sc_{Oct} formed by an Sc^{3+} ion at an octahedral site in the LAG lattice.

Acknowledgments

We would like to thank Johan Th M de Haas, Hans van't Spijker, Matthijs J Knitel and Dennis R Schaart for assistance and the nice atmosphere during the experiments and preparation of the paper. We also thank A A Kiryukhin and D I Melekhov for crystal growth.

This investigation has been supported by The Netherlands Technology Foundation (STW).

References

- [1] Van Eijk C W E, Andriessen J, Dorenbos P and Visser R 1994 *Nucl. Instrum. Methods A* **348** 546
- [2] Batygov S Kh, Voronko Yu K, Kuryukhin A A, Margiani N G, Melekhov D I, Ryskin N N and Tatarintsev V M 1990 *IX All Union Symp. (Leningrad, 1990)* (Leningrad: Academy of Science) p 219
- [3] Valbis Ya A, Volzhenskaya L G, Dubov Yu G, Zorenko Yu V, Nazar I V, Patsagan N I and Pashkovskii M V 1987 *Opt. Spectrosc. (USSR)* **63** 1058
- [4] Rachko Z A and Yansons Ya L 1987 *Opt. Spectrosc. (USSR)* **63** 110
- [5] Batygov S Kh, Voronko Yu K, Kuryukhin A A, Margiani N G, Melekhov D I, Ryskin N N and Tatarintsev V M 1990 *Opt. Spectrosc. (USSR)* **67** 839
- [6] Dorenbos P, de Haas J T M, Visser R, van Eijk C W E and Hollander R W 1993 *IEEE Trans. Nucl. Sci.* **NS-40** 424
- [7] Schotanus P, Dorenbos P, van Eijk C W E and Lamfers H F 1989 *Nucl. Instrum. Methods A* **281** 162
- [8] Schaart D R, Dorenbos P, van Eijk C W E, Visser R, Pedrini C, Moine B and Khaidukov 1994 *J. Phys.: Condens. Matter* to be submitted
- [9] Batygov S Kh, Voronko Yu K, Gribkov I V, Gridin S A, Kuryukhin A A, Margiani N G, Melekhov D I, Ryskin N N and Tatarintsev V M 1990 *Preprint IOFAN*
- [10] Kuznetsov A I, Mürk V V and Namozov B R 1985 *Sov. Phys.-Solid State* **27** 3030
- [11] Gorban I S, Gumenyuk A F, Degoda V Ya and Sizontova E I 1987 *Opt. Spectrosc. (USSR)* **62** 596
- [12] Garmash V M, Ermakov G A, Lubchenko V M and Filimonov A A 1986 *Opt. Spectrosc. (USSR)* **61** 537
- [13] Kuznetsov A I 1992 *Thesis* Ekaterinburg Technical University
- [14] Makhov V N and Ryskin N N 1993 unpublished data
- [15] Volzhenskaya L G, Zorenko Yu V, Patsagan N I and Pashkovskii M V 1987 *Opt. Spectrosc. (USSR)* **63** 135
- [16] Knoll G F 1989 *Radiation Detection and Measurements* (New York: Wiley)

- [17] Dorenbos P, de Haas J T M, van Eijk C W E, Melcher C L and Schweitzer J S 1994 *IEEE Trans. Nucl. Sci.* NS-41 735
- [18] Ashurov M Kh, Voronko Yu K, Osiko V V and Sobol A A 1977 *Phys. Status Solidi a* 42 101
- [19] Dean P J 1973 *J. Lumin.* 7 51
- [20] Valbis Ya A, Gravers V E and Rachko Z A 1966 *Izv. Acad. Sci. (USSR)* 31 661
- [21] Hopfield J J, Thomas D J and Lynch R T 1966 *Phys. Rev. Lett.* 17 312